

PHYSICAL REVIEW A

STATISTICAL PHYSICS, PLASMAS, FLUIDS,
AND RELATED INTERDISCIPLINARY TOPICS

THIRD SERIES, VOLUME 45, NUMBER 10

15 MAY 1992

RAPID COMMUNICATIONS

The Rapid Communications section is intended for the accelerated publication of important new results. Since manuscripts submitted to this section are given priority treatment both in the editorial office and in production, authors should explain in their submittal letter why the work justifies this special handling. A Rapid Communication should be no longer than 3½ printed pages and must be accompanied by an abstract. Page proofs are sent to authors.

Scaling behavior of fluid membranes in three dimensions

David H. Boal and Madan Rao

Department of Physics, Simon Fraser University, Burnaby, British Columbia, Canada V5A 1S6

(Received 21 January 1992)

The scaling behavior of self-avoiding (SA) fluid membranes in three dimensions subject to a bending rigidity κ is studied by Monte Carlo simulation. For $\kappa=0$, open and closed membranes behave like SA branched polymers at large length scales. For arbitrary κ , scaling functions of the combination $y \equiv N^{1/2}/\kappa$ are found to describe the shape variables of closed membranes. The transition from a rigid phase at small y to a SA branched polymer phase at large y is smooth for closed membranes.

PACS number(s): 05.40.+j, 64.70.-p, 82.65.Dp, 87.22.Bt

Over large length scales, fluid membranes such as phospholipid bilayers or surfactant monolayers can be viewed [1] as two-dimensional, self-avoiding, tensionless surfaces governed mainly by their bending rigidity κ . Recently there has been much interest in the shapes and scaling behavior [2] of such surfaces. The scaling of self-avoiding (SA) ring polymers in two dimensions has been the subject of systematic theoretical investigations [3–6]. However, the scaling behavior of polymerized [7–10] and fluid [11,12] surfaces in three dimensions has shown conflicting results.

It is known from one-loop perturbative calculations on non-SA fluid membranes that thermal fluctuations renormalize the bending rigidity, making it smaller at larger length scales [13,14]. Thus non-SA fluid membranes crumple (i.e., the local normals at the surface are uncorrelated) over distances larger than the persistence length $\xi_p \approx a \exp(4\pi\kappa/3)$, where a is a microscopic length parameter. Recently, two simulations have been carried out on SA fluid membranes at zero rigidity. In one simulation [11], the membrane is observed to crumple with a radius of gyration squared R_G^2 which scales like $N^{0.8}$, a scaling behavior predicted on the basis of a Flory argument [7]. In the other simulation [12], $\langle R_G^2 \rangle$ scales like N^1 , and the membrane behaves like a SA branched polymer (SABP) in three dimensions [15,16]. Glaus [17] has shown that

self-avoiding random surfaces also belong to the universality class of branched polymers.

In the present paper, we perform Monte Carlo simulations of open and closed SA fluid membranes embedded in three dimensions. Our algorithms, used elsewhere [18] to examine the open-closed transition of fluid membranes, are slightly different from Refs. [11,12]. Our results favor branched polymer scaling for both open and closed vesicles at $\kappa=0$. At intermediate κ , a scaling ansatz shows that closed configurations are governed by an unstable, rigid, $\kappa=\infty$ fixed point. This leads to the main conclusion of the paper—SA fluid membranes with finite κ scale like SABP's for sufficiently large systems.

As in many previous simulations, we represent the membrane by a two-dimensional manifold consisting of a fixed number N of hard spherical beads (or vertices) linked together by straight flexible tethers. The tethers have a maximal length chosen to prevent self-intersection of the membrane. Because of the tethers, the total area of the membrane is not a constant and can change by up to 50% around the mean. A convenient choice for a discrete Hamiltonian governing the bending energetics of the membrane is

$$\beta H = \kappa \sum_{\langle i,j \rangle} (1 - \mathbf{n}_i \cdot \mathbf{n}_j) \quad (1)$$

where β is the inverse temperature and each \mathbf{n} is a unit vector normal to the plane formed by three vertices which are all nearest neighbors to one another. The sum is over \mathbf{n} 's whose defining plaquettes share a common tether. The self-avoidance constraint is imposed by using step functions: The vertices are infinitely repulsive at distances less than the bead diameter a (for all vertex pairs) or greater than $\sqrt{3}a$ (for vertices connected by tethers).

A set of appropriately weighted sample configurations is generated using the usual Metropolis Monte Carlo technique in which trial moves are made on the vertex positions and connectivity. In our simulation of open membranes, we use a label which distinguishes between the external vertices defining the edge of the sheet, and the internal vertices not at the edge. Similarly, an external tether is connected to two external vertices, while an internal tether is connected to at least one internal vertex. The closed membrane (vesicle) simulations contain no external vertices or tethers.

A sweep across the membrane involves the following steps: (i) An attempt is made to change the position of each vertex by choosing another position randomly from within a cubic box of length $2l$ to the side centered on the old position. (ii) An attempt is made to reconnect every internal tether following the procedure of Baumgartner and Ho [11] to simulate fluidity. In this procedure, an attempt is made to cut a tether and replace it with a tether connecting the two "opposite" vertices which (along with the vertices at the ends of the original tether) define the two triangles having the original tether in common. This procedure conserves the number of tethers and plaquettes.

If the membrane is an open sheet, then there are external vertices and tethers present which require additional moves: (iii) An attempt is made to remove each external tether, thus converting two internal tethers into new external tethers and reducing the overall number of tethers by one. (iv) An attempt is made to connect two next-nearest-neighbor external vertices with a new external tether, thus converting two external tethers to internal tethers and increasing the overall number of tethers by one. Each trial move is accepted or rejected according to the Boltzmann weight $\exp(-\beta\Delta H)$. Unlike a number of previous simulations of open membranes, we do not fix the number of vertices defining the perimeter.

The following algorithmic steps forbid the formation of holes in the membrane: (i) A given vertex must have at least three tethers connecting it. (ii) An external vertex may not be connected by more than two external tethers. (iii) The external vertices and tethers define only a single continuous boundary. New boundaries in the interior of the membrane are forbidden. Further, at each reconnection step the algorithm forbids a given tether to be common to more than two triangular plaquettes. This ensures that the topology of the membrane is not changed. (That is, the membrane is defined only by triangles, and all triangles formed by three vertices which are nearest neighbor to each other live on the surface. No tether is common to more than two triangles).

Either 100 or 200 sample configurations are generated at each (κ, N) combination. Each configuration is separated by a "Rouse time" $\tau = N/l^2$ Monte Carlo

sweeps. The equilibration time is approximately equal to the Rouse time for non-SA polymerized membranes [7], but is approximately a factor of 2 longer than the Rouse time for SA polymerized membranes with $N=300$ or so [8]. For fluid membranes, we visually estimate the equilibration time to be 10–15 Rouse times for the system sizes considered. Hence, each initialization is allowed to relax for 30τ before sample collection commences. For the largest system sizes, between 5 and 10×10^6 attempted moves are made for each vertex and bond, comparable to the number of moves used in Refs. [11,12].

Several checks are made on the $N=542$ membranes for equilibration. For $\kappa=0$, observables are calculated both from the entire 200τ configuration set and from the last 50τ configurations only. The results agree within statistical errors. For $\kappa=1.5$ and 2, separate samples are generated from different initializations [130 τ configurations from a flat pancake start and (65–110) τ configurations from the last configuration at $\kappa=1$]. Again, observables calculated with these different data sets agree within errors.

From the parameters in the Hamiltonian, one can construct two natural length scales: the rigidity length $L_\kappa = \kappa a$ (related to the persistence length ξ_p) and the areal length $L_A = N^{1/2}a$. We are interested in the scaling behavior of geometrical quantities like the mean volume $\langle V \rangle$ (for closed membranes), the mean circumference $\langle C \rangle$ (for open membranes), and the mean square radius $\langle R_G^2 \rangle$ as N becomes large and κ ranges over all nonnegative values.

At $\kappa=0$, we expect the membrane to be very flexible and $\xi_p \approx O(a)$. Figure 1 shows typical open (a) and closed (b) configurations with ramified arms which resemble a branched polymer. We expect that the geometrical quantities scale asymptotically as $\langle R_G^2 \rangle = R_0^2 N^\nu$, $\langle V \rangle = V_0 N^\mu$, and $\langle C \rangle = C_0 N^\lambda$. The behavior of $\langle R_G^2 \rangle$ and $\langle V \rangle$ is shown in Fig. 2. We find that for open membranes $\nu = 1.11 \pm 0.05$ and $\lambda = 1.01 \pm 0.05$ at $\kappa=0$. This is consistent with SABP behavior [17] where $\nu = \lambda = 1$ and with Ref. [12]. The values of the exponents should not depend on whether the membrane is open or closed. However, for closed membranes we find that $\nu = 0.92 \pm 0.05$ and $\mu = 1.18 \pm 0.05$. The value of μ is consistent with Ref. [11] but is significantly larger than the BP result [17] $\mu = 1$. We believe that the origin of this discrepancy lies in the algorithms of the simulations, and we return to this question below.

When κ becomes infinite, fluctuations in the shape are suppressed and the membrane transforms into a rigid geometrical object. For closed membranes we expect the shape to be a rigid sphere, where $\langle R_G^2 \rangle = R_\infty^2 N$ and $\langle V \rangle = V_\infty N^{3/2}$. Such spherical configurations are seen in the simulations (see Fig. 1 in Ref. [18]). For open membranes we expect a flat, rigid shape with an arbitrarily long boundary due to entropy. We conjecture that such a shape scales as a two-dimensional SABP with [19] $\nu = 1.28$.

What is the scaling behavior at intermediate values of κ ? In analogy with the analysis of polymers in two dimensions [3,4], we conjecture that the shape of the closed membrane at intermediate κ is governed by an unstable

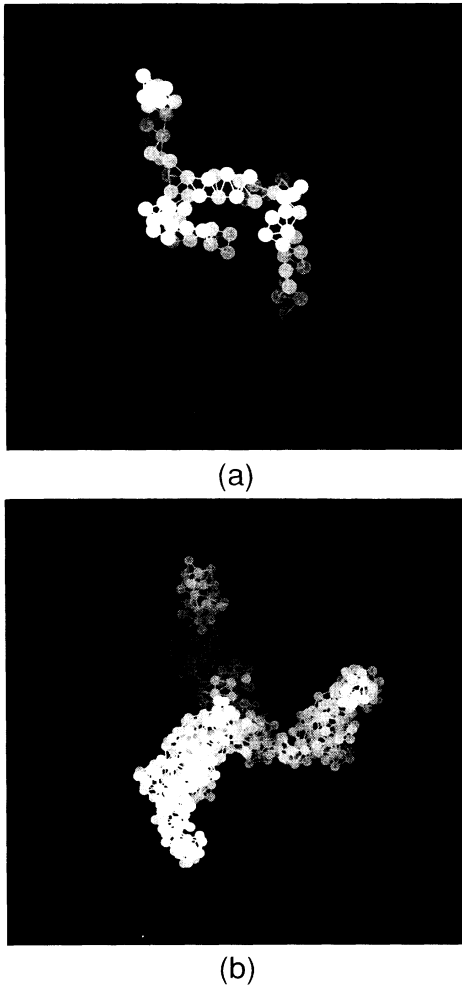


FIG. 1. Sample configurations for (a) open and (b) closed membranes. (a) $\kappa=0, N=91$; (b) $\kappa=0, N=542$.

rigid fixed point at $\kappa=\infty$, where self-avoidance is irrelevant. At this zero-temperature fixed point the scaling fields do not have any anomalous dimensions. This immediately suggests that the correct scaling variable should be $y=N^{1/2}/\kappa$ which is the ratio of the two length scales L_A/L_κ . For closed membranes we postulate that the shape scales as $\langle R_G^2 \rangle \equiv R_\infty^2 N \Phi(y)$ and $\langle V \rangle \equiv V_\infty N^{3/2} \Theta(y)$ with the normalization $\Phi(0)=\Theta(0)=1$ to get the correct scaling for the rigid membrane at $\kappa=\infty$. This fixes the nonuniversal metrical factors R_∞ and V_∞ . If the scaling formulation is “complete” it should describe the SABP configurations at $y \rightarrow \infty$. Thus one expects, as $y \rightarrow \infty$,

$$\begin{aligned} \Phi(y) &\approx \Phi_\infty / y^{2-2\nu}, \\ \Theta(y) &\approx \Theta_\infty / y^{3-2\mu}, \end{aligned} \tag{2}$$

with exponents ν and μ given by the three-dimensional SABP values. Thus we expect a smooth crossover from the closed rigid $\kappa=\infty$ phase to the $\kappa=0$ SABP phase.

Figure 3 shows a log-log plot of $\langle V \rangle / N^{3/2}$ vs y for N ranging from 74 to 542. The collapse of the data to a single scaling function is clear; the appearance of the collapse can be improved by the introduction of shift parameters to

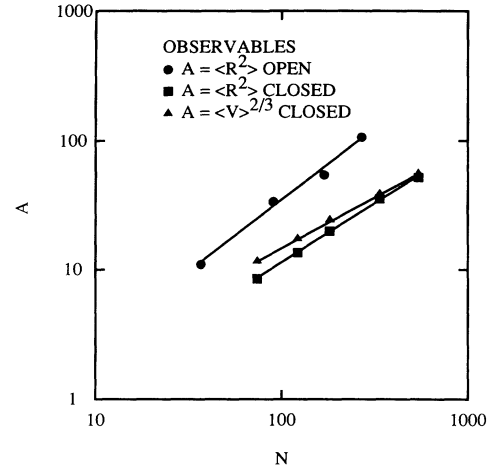


FIG. 2. Scaling behavior for open and closed configurations at $\kappa=0$. The data are shown for $\langle R_G^2 \rangle$ (open and closed) and $\langle V \rangle^{2/3}$ (closed). The uncertainty in the data is 7%. The straight lines are fits to the data discussed in the text.

account for finite-size [4] and other effects. A similar scaling behavior in accord with Eq. (2) is observed for $\langle R_G^2 \rangle$. It appears that $\langle R_G^2 \rangle / N$ is almost a constant for all values of y .

We see from Fig. 3 that the curves for fixed N peel off from a limiting form (which goes to zero as $y \rightarrow \infty$) when κ decreases, since $\langle V \rangle = V_0 N^\mu$ at zero κ . The behavior of the $N=542$ vesicle is highlighted in the figure. The limiting form corresponds to the asymptotic expression (2). The exponent μ can be extracted from the slope of the segment in the intermediate y regime in Fig. 3. Parametrizing this segment as $y^{-\rho}$, we expect $\rho=3-2\mu$ as N becomes large. From the figure, the value of ρ at each N (around $y=10-20$) increases with N : $\rho=0.6$ ($N=74$), 0.75 ($N=122$), 0.91 ($N=182$), and 1.06 ($N=542$) with a 10% uncertainty. Clearly, the values of ρ at large N cluster around unity. In fact, if one extrapo-

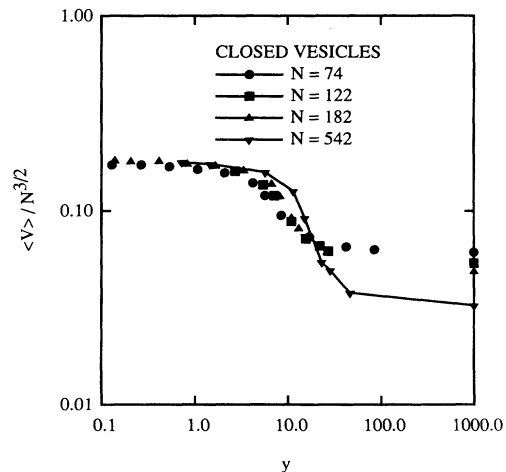


FIG. 3. Scaling analysis of the volume for closed vesicles. The reduced volume $\langle V \rangle / N^{3/2}$ is shown as a function of $y=N^{1/2}/\kappa$. The $N=542$ data are linked by a solid line for clarity. Data for $\kappa=0$ are nominally plotted at $y=1000$.

lates ρ to $N = \infty$ using $\rho(N) = \rho(\infty) + B/N$ where B is a fit parameter, then $\rho(\infty) = 1.1 \pm 0.1$. This allows us to distinguish between branched polymer scaling, for which $\rho(\infty) = 1$, and the results of Ref. [11] ($\mu = 1.2$) for which $\rho(\infty) = 0.6$. Hence, we argue that the scaling analysis favors the SABP exponent even though our simple analysis of $\log\langle V \rangle$ vs $\log N$ in Fig. 2 gives $\mu = 1.2$, in agreement with Ref. [11].

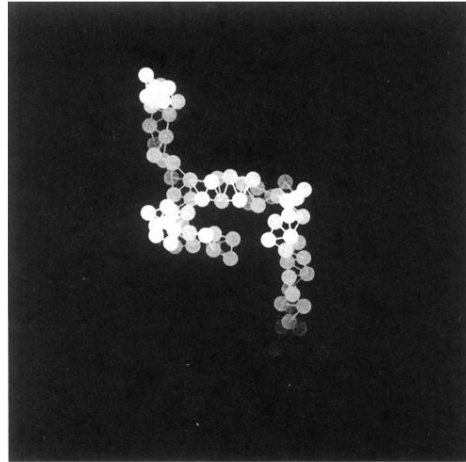
We now address the issue of why our value of μ for closed membranes at $\kappa = 0$ is larger than that expected for SABP's. In Ref. [12], configurations with long thin ramified structures of cross sectional width $O(a)$ appear at modest values of N . Such structures are prevented in our simulations at small N . In our simulations, the membrane surface is defined by triangles, and *all* triangles defined by three vertices which are nearest neighbors to each other live on the surface. Thus, a cross section taken through an arm of a branched polymer configuration shows a minimum of four vertices in our simulation. In contrast, in Ref. [12] a separate label is kept for the surface triangles, thus allowing a given tether to be common to three triangles, only two of which are surface triangles. A cross section through a branched polymer arm in Ref. [12] shows many regions where only three vertices define

the arm. In other words, the lower length scale cutoff is larger in our simulations than in Ref. [12]. Hence, we must go to larger values of N to observe the same branched polymer configurations as observed in Ref. [12].

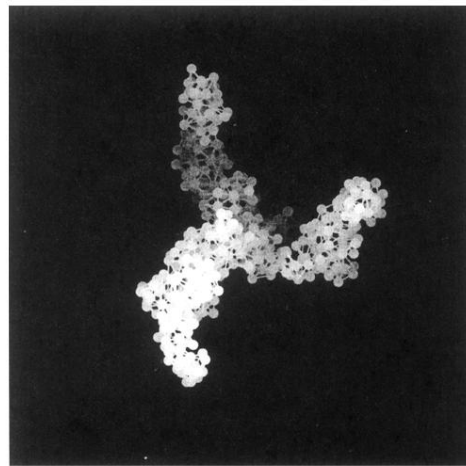
In conclusion, we have investigated the scaling behavior of the shapes of self-avoiding fluid membranes in three dimensions as a function of κ . We find that at $\kappa = 0$, both the open and closed membranes behave like a three-dimensional SABP at large N . The shapes of closed membranes at nonzero κ can be described in terms of the scaling variable $y = N^{1/2}/\kappa$. This scaling behavior is governed by an unstable rigid fixed point at $\kappa = \infty$. We find that there is a large regime in y space $(0, \infty]$ over which the scaling form holds. As in Ref. [4], we speculate that the reason for this might be due to the presence of nonlinear scaling fields. Thus, at any finite value of κ the membrane exhibits SABP behavior at large length scales. This implies that the SA fluid membrane is crumpled at all nonzero temperatures.

This work is supported in part by the Natural Sciences and Engineering Research Council of Canada. We thank D. Kroll and G. Gompper for extensive discussions and simulation comparisons.

-
- [1] *Physics of Amphiphilic Layers*, edited by J. Meunier, D. Langevin, and N. Boccardo (Springer-Verlag, Berlin, 1987).
- [2] *Statistical Mechanics of Membranes and Surfaces*, edited by D. R. Nelson, T. Piran, and S. Weinberg (World Scientific, Singapore, 1989); R. Lipowsky, *Nature (London)* **349**, 475 (1991).
- [3] S. Leibler, R. R. P. Singh, and M. E. Fisher, *Phys. Rev. Lett.* **59**, 1989 (1987).
- [4] C. J. Camacho, M. E. Fisher, and R. R. P. Singh, *J. Chem. Phys.* **94**, 5693 (1991).
- [5] B. Duplantier, *Phys. Rev. Lett.* **64**, 493 (1990).
- [6] D. H. Boal, *Phys. Rev. A* **43**, 6771 (1991).
- [7] Y. Kantor, M. Kardar, and D. R. Nelson, *Phys. Rev. Lett.* **57**, 791 (1986).
- [8] M. Plischke and D. H. Boal, *Phys. Rev. A* **38**, 4943 (1988); D. Boal, E. Levinson, D. Liu, and M. Plischke, *ibid.* **40**, 3292 (1989).
- [9] R. Lipowsky and M. Girardet, *Phys. Rev. Lett.* **65**, 2893 (1990).
- [10] S. Komura and A. Baumgartner, *Phys. Rev. A* **44**, 3511 (1991).
- [11] A. Baumgartner and J.-S. Ho, *Phys. Rev. A* **41**, 5747 (1990).
- [12] D. M. Kroll and G. Gompper, *Science* (to be published).
- [13] W. Helfrich, *J. Phys. (Paris)* **46**, 1263 (1985).
- [14] L. Peliti and S. Leibler, *Phys. Rev. Lett.* **54**, 1690 (1985).
- [15] T. C. Lubensky and J. Isaacson, *Phys. Rev. A* **20**, 2130 (1979).
- [16] G. Parisi and N. Sourlas, *Phys. Rev. Lett.* **46**, 871 (1981).
- [17] U. Glaus, *J. Stat. Phys.* **50**, 1141 (1988).
- [18] D. Boal and M. Rao (unpublished).
- [19] B. Derrida and D. Stauffer, *J. Phys. (Paris)* **46**, 1623 (1985).



(a)



(b)

FIG. 1. Sample configurations for (a) open and (b) closed membranes. (a) $\kappa=0$, $N=91$; (b) $\kappa=0$, $N=542$.